Environment International 132 (2019) 105127

Contents lists available at ScienceDirect

Environment International

journal homepage: www.elsevier.com/locate/envint

Accurate quantification and transport estimation of suspended atmospheric microplastics in megacities: Implications for human health

Kai Liu, Xiaohui Wang, Nian Wei, Zhangyu Song, Daoji Li*

State Key Laboratory of Estuarine and Coastal Research, East China Normal University, 500 Dongchuan Road, Shanghai 200062, China

ARTICLE INFO

Handling Editor: Xavier Querol

Keywords:
Suspended atmospheric microplastics
Sampling methodology
Transport
Impact

ABSTRACT

Although atmospheric microplastics have been found to be ubiquitous even on untraversed mountains and have potential impacts on human health, little information concerning their sampling methodology and transport is currently available. Until a realistic quantification of suspended atmospheric microplastics (SAMPs) is obtained, however, any potential health risk assessment for this pollutant will be open to criticism for using an ambiguous dataset. To address this knowledge gap, in May 2019 a trial experiment was performed to explore the potential relationship between sampling volume and SAMP abundance. A significant logarithmic regression between SAMP abundance and the sampling volume of filtrated air was found and the sufficient volume of filtrated air for accurate SAMP quantification was recommended. Investigation results indicated that fibrous and fragment-shaped SAMPs comprised 91% of all of the identified synthetic particles. Interestingly, for the first time, plastic microbeads were also observed in the collected air, constituting 9% of the all of the SAMPs by quantity. Spectral analysis revealed that these SAMPs consisted of polyethylene terephthalate (PET), epoxy resin (EP), polyethylene (PE), alkyd resin (ALK), rayon (RY), polypropylene (PP), polyamide (PA), and polystyrene (PS). PET, EP, PE, and ALK constituted the majority (90%) of all of the polymer types, with quantitative percentages of 51%, 19%, 12%, and 8%, respectively. Based on our numerical modeling simulation, the approximate transport flux of SAMPs during June in Shanghai was estimated, ranging from 9.94×10^4 n/(m·d) to 6.52×10^5 n/(m·d), with a mean of $3.00 \pm 1.58 \times 10^5$ n/(m·d). The goal of our study was to provide an essential methodological aid for the accurate determination of SAMPs in the environment and a better understanding of terrestrial microplastic transport in megacities.

1. Introduction

Microplastics (MPs, typically with size < 5 mm along its longest dimension), as an emerging organic pollutant, have been drawing increasing global attention due to their ubiquity (Law and Thompson, 2014; Ostle et al., 2019) and potential threat to human health (Carbery et al., 2018). Ingested MPs by terrestrial (Zhao et al., 2016) and aquatic (Su et al., 2019) organisms have been widely reported and implications of trophic transfer have also been found in many species (Setälä et al., 2014; Zhao et al., 2018). In addition to trophic transfer via the food chain or web, recent research has revealed that microplastics may possibly have a negative influence on human health via inhalation (Prata, 2018). C. Liu et al. (2019) collected indoor and outdoor dust from 39 cities in China and evaluated the potential human health impacts. It was roughly estimated that 17,300 ng/kg-bw of fibrous MPs of PET composition are inhaled daily by children, indicating the potential risk of these airborne particles. Similarly, Abbasi et al. (2019) investigated the distribution and potential health impacts caused by SAMPs from Asaluyeh County, Iran. Modeling results revealed that 5–15 particles and 2–7 particles were ingested daily by construction workers and children, respectively, under the acute exposure scenario. Both of these studies stressed the importance of SAMPs and their potential health impacts on humans. However, until realistic SAMP abundance levels are obtained, any potential ecological or health risk assessment for SAMPs will potentially be prone to either underestimation or overestimation.

Recently, even the polar region, in which there are few anthropogenic activities, has proven to be contaminated by MPs, with considerable concentrations of MPs discovered in ice cores, especially fibrous MPs (Peeken et al., 2018). The latest findings from the aforementioned research imply that fiber-shaped MPs from textile sources could be derived from the terrestrial environment via air circulation. Few studies concerning SAMP pollution are currently available, however, and SAMP distribution and transport in the urban

* Corresponding author.
E-mail address: daojili@sklec.ecnu.edu.cn (D. Li).

https://doi.org/10.1016/j.envint.2019.105127
Received 19 July 2019; Received in revised form 17 August 2019; Accepted 25 August 2019
Available online 02 September 2019

environment remain largely unknown. Although some researchers have investigated SAMP pollution in urban areas, a detailed comparison among these studies was inadequately performed due to the random and arbitrary sampling of SAMPs. A huge knowledge gap exists between the potential health assessment and the realistic quantification of SAMPs, of which reliable sampling methodology plays a crucial role. However, reliable and authentic sampling methods for the accurate quantification of SAMPs have yet to be well established and are urgently needed.

Shanghai is a global financial megacity, recognized as being both densely populated (3814 residents/km^2, *Shanghai Statistical Yearbook*, 2018) and heavily polluted (Kan et al., 2012). The intensive anthropogenic activities of this area can produce tremendous numbers of MPs, with the potential to generate and accumulate numerous SAMPs. Nevertheless, the occurrence, transport, and fate of SAMPs in this megacity remain largely unknown. To address this issue, the accurate quantification of SAMPs and their transport patterns was investigated in Shanghai. The goal of this study was to provide a methodological aid to improve our understanding of the source, transport, and fate of MPs in the environment. We attempted to provide an inclusive and detailed framework that can be utilized in the potential impact assessment of MPs on humans and climate.

2. Material and methods

2.1. Study area and sampling volume verification

In this study, air samples of 1, 2, 3, 5, 9, 14, 18, 30, 72, 100 and 144 m^3 were continuously filtrated in triplicate at the southeast corner of the roof (38 m above the ground) of the State Key Laboratory of Estuarine and Coastal Research (SKLEC), East China Normal University (Fig. 1) during May and June 2019.

A sampling protocol identical to that described in K. Liu et al. (2019a) was adopted. During this investigation, a KB-120F particulate sampler (Jinshida, Qingdao, China) was utilized to collect SAMPs. The general procedure was as follows: GF/A glass microfiber filters (Whatman, UK), each with a 1.6 μm pore size and a 90 mm diameter, were carefully placed in an aluminum alloy impactor using stainless steel tweezers. Next, the impactor was inserted into the upper part of the sampler and gently screwed in. The instrument was then set to delayed sampling (1 min) in order to avoid any contamination from the experimenter. For each sampling, the necessary pressure correction on the filter was performed by the system software so as to accurately quantify the volume of filtrated air. Once the sampling was finished, the filter was carefully plucked out and temporarily stored in clean-air sampling cassettes within an SW-CJ-1FB ultra-clean worktable (Sujing, Shaoxing, China).

In order to avoid contamination from the resuspension of ground dust, the aluminum alloy tripod of the instrument was placed horizontally on an iron platform (1.28 m above the roof) and then adjusted to 1.70 m above the iron platform in order to minimize the airflow interference from the building. Meanwhile, environmental factors at the same height were simultaneously documented every 6 min using a 5500 L portable weather meter (Kestrel, U.S.A.).

2.2. MPs verification

2.2.1. Particle inspection

Suspicious microplastics on the filters were observed and photographed under stereomicroscopy (Leica M165 FC, Germany) equipped with a Leica DFC 450C camera.

2.2.2. MP identification

A Nicolet iN10 Micro Fourier Transform Infrared Spectrometer (Thermo Fisher Scientific, U.S.A.) equipped with a mercury cadmium telluride (MCT) detector was chosen to verify these isolated microplastics (K. Liu et al., 2019b). Ample liquid nitrogen was needed to cool the MCT detector prior to its use, and another 30–40 min was recommended by the instruction manual to help stabilize and improve the signal. Mid-infrared waves (4000–675 cm^{-1}) were used to co-scan marked SAMPs 16 times at a resolution of 4 cm^{-1} and spectra were obtained in transmission mode. Background interference (i.e., CO_2 and

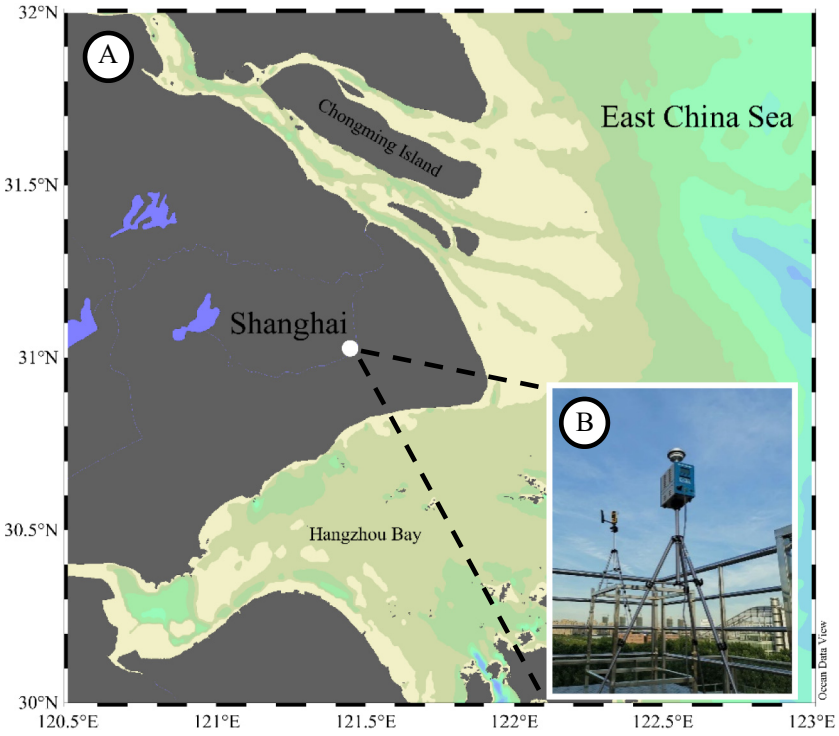

Fig. 1. The study area (A) and sampling device (B) used in this investigation.

H_2O) had to be calibrated prior to each analysis. The spectra were then analyzed using OMNIC 9 software and compared with the OMNIC spectra library. Targeted substances were only considered to be plastic materials when the match confidence was > 60%.

2.3. Transport flux of SAMPs

Driven by wind, aerial SAMPs can be transported to remote areas and are a consistent source of marine MP pollution. In this study, a rough estimation of the horizontal transport flux of SAMPs was calculated as follows:

$$Flux(\text{SAMPs}) = \int_0^{h_1} N_\delta w_\theta d_z \quad (1)$$

where N_δ, w, and z represent the SAMP abundance (n/m^3) (items per cubic meter of air), the horizontal wind speed (m/s) in the θ direction, and approximate sampling height (40 m), respectively.

2.4. Quality assurance

Strict measures were used to present the external contaminations. Firstly, GF/A glass microfiber filters were carefully wrapped with aluminum foil and then combusted at 450 °C for 4 h prior to use as Zhao (2017) described. Secondly, all sample cassettes were washed with pre-filtrated Milli-Q water (resistivity: 18.2 MΩ·cm, 25 °C) and air-dried in an SW-CJ-1FB type ultra-clean worktable (Sujing, Shaoxing, China) with a vertical wind of 0.6 m/s. Thirdly, SAMPs verification was performed in an ultra-clean stainless steel room (K. Liu et al., 2019b) and lab coats (100% cotton) and nitrile gloves were worn during the whole procedure. In addition, procedure blank was performed during sampling and identical process was adopted to examine the potential contamination.

2.5. Statistical analysis

Data analysis was performed using SPSS 23.0 software and all of the graphs displayed in this manuscript were generated by Origin Pro 2017. Significant difference was reported at the $P < 0.05$ level. Value was present with mean ± standard deviation (SD) unless otherwise specified.

3. Results

3.1. SAMP quantification

No contamination from the procedure blank was found during the analysis. SAMPs were ubiquitous in the surroundings, ranging from 0 to 2 n/m^3, with a mean value of 0.41 n/m^3. Both higher average SAMP abundance (0.27–1.33 n/m^3) and variation (SD: 0.29–0.58) were found in 1–5 m^3 sampled air, while these values tended to stabilize when the volume of the filtrated air increased (Fig. 2-A).

Interestingly, statistical analysis revealed that the sample volume of filtrated air had a significant influence on the SAMP quantification. A logarithmic relationship between the sampling volume and mean SAMP abundance was discovered (R = 0.87, $P = 0.001 < 0.01$), as expressed in the following formula:

$$A = 0.93 - 0.2 \ln v \quad (2)$$

where A and v represent the average SAMP abundance (n/m^3) and the volume of the filtrated air (m^3), respectively. Furthermore, we also analyzed the correlation between the abundance of specifically shaped SAMPs and the sampling volume of air. A significant logarithmic regression between the average abundance and the volume of the sampled air was also found for the fibrous SAMPs ($A = 0.64–0.16 \ln v$, R = 0.79, $P = 0.004 < 0.01$) (Fig. 2-B). However, fragment-shaped SAMPs appeared to be heterogeneous, with a random distribution and no discernible statistical regression (linear: R = 0.47, $P = 0.15 > 0.05$; logarithmic: R = 0.39, $P = 0.24 > 0.05$) (Fig. 2-C).

Overall, with higher volumes of filtrated air (Fig. 2-A), SD of SAMPs abundance tended to decease (from 0.58 to 0.02) and approximately stabilized (0.02–0.03) when sampling volume was higher than 72 m^3. Compared to higher SD variation by smaller sampling volume, more stable and authentic MPs abundance could be achieved when sufficient sample capacity (> 72 m^3) was obtained. Thus, a filtrated air sampling volume of at least 70 m^3 is required and recommended for SAMP quantification. Based on the sufficiently-sized samples, the accurate SAMP abundance in Shanghai during June varied from 0.05 to 0.07 n/m^3, with a mean of 0.06 ± 0.01 n/m^3.

3.2. Morphological and chemical features of SAMPs

Then, 146 of the 188 sample particles were confirmed to be plastic materials by spectral analysis; the typical SAMPs are presented in Fig. 3. Categorized by physical appearance, these SAMPs were mainly comprised of fibrous and fragment-shaped MPs, with numerical proportions of 43% and 48%, respectively. Interestingly, plastic microbead (n = 13) were also discovered during the sampling, constituting 9% of all SAMPs by quantity.

The size of every SAMP particle was measured and found to vary from 12.35 to 2191.32 μm, with an average value of 246.52 μm (Fig. 4-A). Generally, as SAMP size decreased, the quantity gradually increased, with numerically higher amounts of smaller-sized SAMPs typically found. A larger mean size (428.81 μm) was observed for fibrous SAMPs, followed by the fragmented and microbead-shaped SAMPs, with average sizes of 121.44 μm and 36.59 μm, respectively (Fig. 4-B, C, and D, respectively).

Meanwhile, these SAMPs also exhibited a colorful appearance. Eleven different colors were observed: white, pink, black, red, yellow, gray, blue, green, transparent, purple, and brown (Fig. 4-A). Black, white, and transparent SAMPs made up over half (56%) of the total identified particles by number, of which black SAMPs comprised 48%, followed by white and transparent particles.

Further spectral analysis revealed that these SAMPs consisted of polyethylene terephthalate (PET), epoxy resin (EP), polyethylene (PE), alkyd resin (ALK), rayon (RY), polypropylene (PP), polyamide (PA), and polystyrene (PS). PET, EP, PE, and ALK constituted the majority (90%) of all of the polymer types, with quantitative percentages of 51%, 19%, 12%, and 8%, respectively. In Fig. 4-A, the top 4 polymer types in terms of quantity were included and a distinct polymer composition was found among the variously-shaped SAMPs. Fibrous SAMPs made up of PET ranked first of all fiber-shaped SAMPs, with a particle proportion of 87%, followed by PE and RY (Fig. 4-B). Meanwhile, more EP-type SAMPs were verified in both the fragmented and microbead-shaped MPs, with numerical percentages of 27% and 69%, respectively (Fig. 4-C and D). This large difference could possibly reflect source differences, since fiber-shaped SAMPs likely originated from the emission of textile materials, while fragmented and microbead SAMPs were possibly derived from other sources.

3.3. Influence factors and transport flux of SAMPs

Principal component analysis (PCA) from the unconstrained model has been applied to explore the relationship between weather conditions and SAMP abundance (C. Liu et al., 2019; K. Liu et al., 2019a, 2019b). In this study, it was also used to determine the inner connection between environmental factors and SAMP distribution (Fig. 5).

Based on the previous trial experiment, we only used the realistic SAMP data from the sampling volumes of the filtrated air > 70 m^3. 81% of the total variance from the sampling stations could be explained with 2 principal component axes (PC1 and PC2), of which PC1 contained 64% of the variable loading of the environmental factors, while

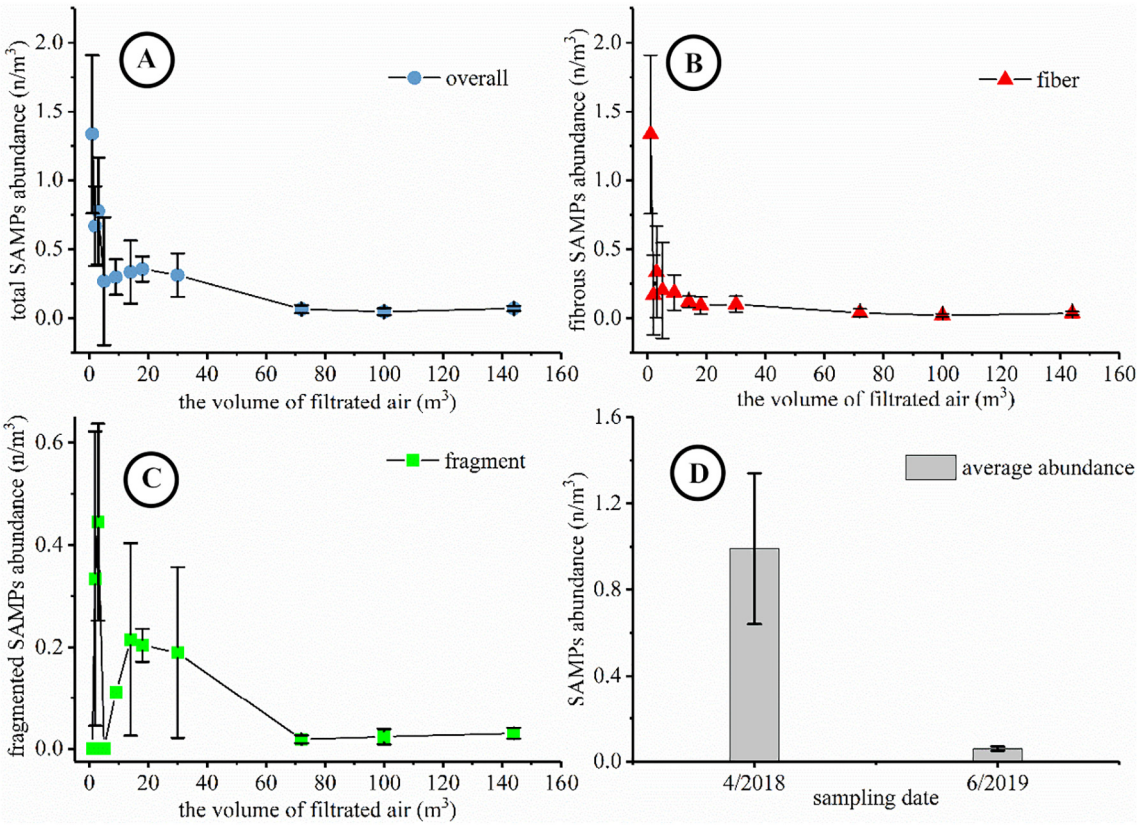

Fig. 2. Relationship between the total (A), fibrous (B), and fragmented (C) SAMP abundance and the volume of sampled air; annual variation of aerial SAMP abundance in Shanghai (D). In the figure, all of the values are illustrated as mean ± standard deviation (n = 3). In Fig. 2-D, SAMPs collected during April 2018 were sampled at the similar height of 33 m in the Putuo District of Shanghai (K. Liu et al., 2019a).

PC2 contained 18%. For the detailed loading of the environmental parameters on every axis, please refer to Appendix A. The relative distance between the circles indicates the differences between the sampling compositions. In addition, although some positive (acute angle between the loading arrows) and negative (obtuse angle between the loading arrows) relationships between SAMP abundance and other environmental factors were observed, no statistically significant regression was found. However, these results could still help reveal SAMP distribution and transport in megacities. For example, the approximate positive correlation between SAMP abundance and wind direction suggested an important source of these airborne particles. Intriguingly, a roughly positive relationship between SAMP abundance and barometric pressure was observed, implying that a portion of the SAMPs could be associated with vertical transport, in addition to lateral movement.

Further spatial analysis could provide more specific identification of SAMP sources as well as the influence of environmental factors on SAMP distribution. Our findings indicated that the Fengxian District (1681 residents/km^2) and the Pudong New Area (4567 residents/km^2) (*Shanghai Statistical Yearbook*, 2018) in the southeast part of the city, both with relatively high population densities (particularly Pudong), could potentially contribute to SAMP pollution (Fig. 6-A). Theoretically, higher horizontal wind speeds would probably carry more SAMPs downwind than lower wind speeds. However, an approximate negative correlation between SAMP abundance and wind speed was found (Fig. 5). The inconsistency of SAMP abundance and wind speed in a particular direction demonstrated that another vital pathway of atmospheric MPs and SAMPs from higher altitudes possibly contributed a portion of the observed particles (Fig. 6-B). This hypothesis was further supported by the generally positive relationship between barometric pressure and SAMP abundance (Fig. 6-D).

Given the distinct environmental behavior of MPs as a function of their morphological characteristics, in this study fibrous and fragment-shaped SAMPs were separately considered in order to gain clear insight into the SAMP transport. Based on our preliminary modeling, the transport flux of the total SAMPs in Shanghai during June ranged from 1.15 to 7.54 n/(m·s), with a mean value of 3.47 ± 1.83 n/(m·s). The transport fluxes for fibrous and fragmented SAMPs were 0.58–2.41 n/(m·s) and 0.58–4.31 n/(m·s), with averages of 1.62 ± 0.72 n/(m·s) and 1.45 ± 1.16 n/(m·s), respectively. Although further analysis revealed no significant difference between the transport fluxes of fibrous and fragment-shaped SAMPs (Kruskal-Wallis test, $\chi^2 = 8$, $df = 8$, $P = 0.43 > 0.05$), distinct transport patterns for these different-shaped SAMPs in specific directions were observed via spatial analysis (Fig. 6). Apparently, fibrous SAMP flux peaked in both the south and east directions (Fig. 6-E), while higher flux for fragment-shaped SAMPs was found in the southerly direction (Fig. 6-F).

4. Discussion

4.1. Source and distribution of SAMPs

Ubiquitous SAMPs were discovered in the megacity of Shanghai and their accurate quantification was obtained. Potential source of SAMPs could be speculated according to physical and chemical property (Table 1).

A considerable amount of SAMPs, especially plastic microfibers, are possibly generated by the breakdown of textile materials (e.g., clothes, blankets, and curtains) when subjected to mechanical abrasion and UV irradiation (Song et al., 2017). For example, fibrous SAMPs could be generated through the drying of clothes, blankets, and curtains (K. Liu et al., 2019a). In Shanghai, residents tend to dry their clothing by

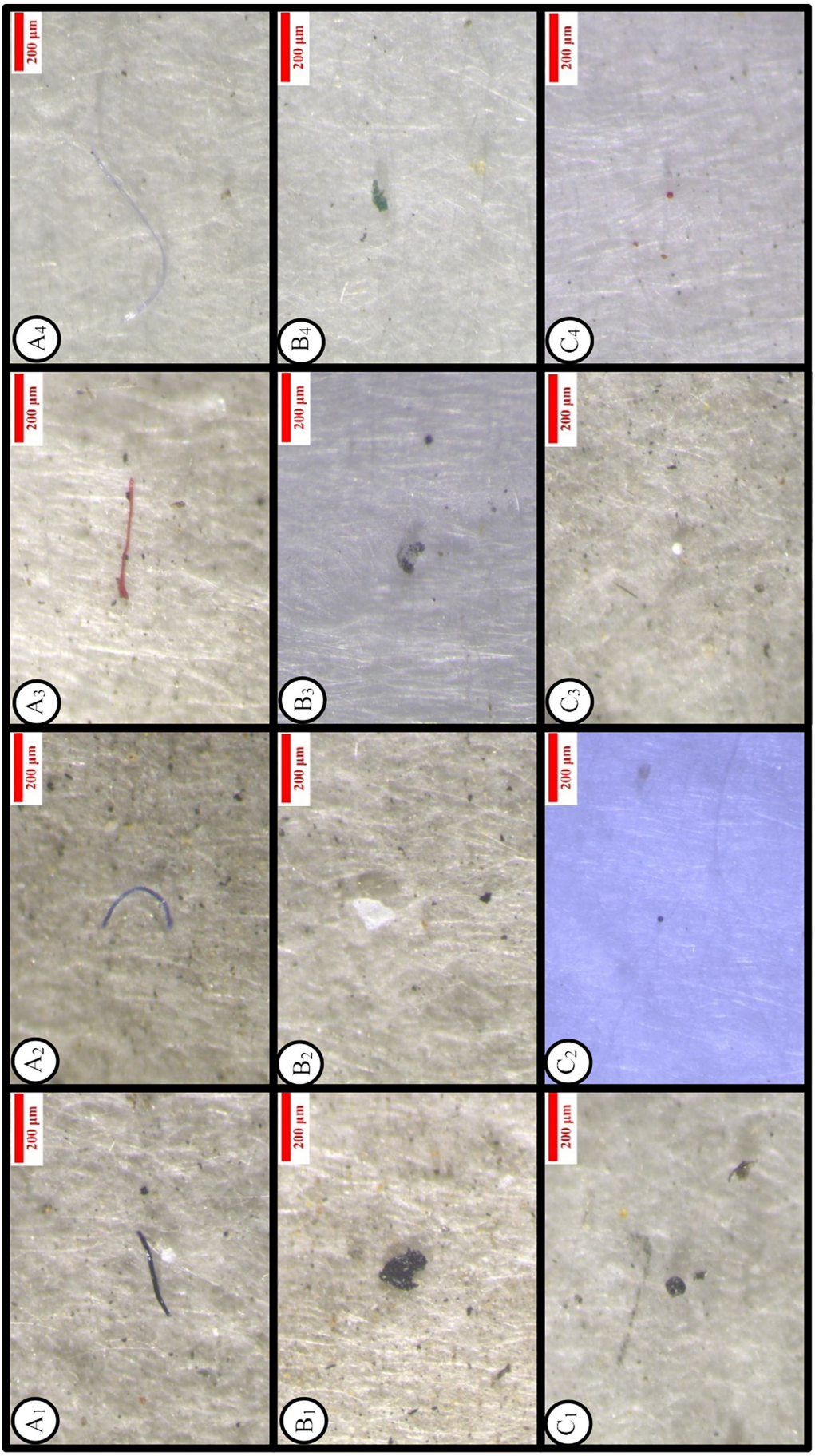

Fig. 3. Photographs of typical microplastics from the collected air samples. A_1–A_4: fibers; B_1–B_4: fragments; C_1–C_4: microbeads.

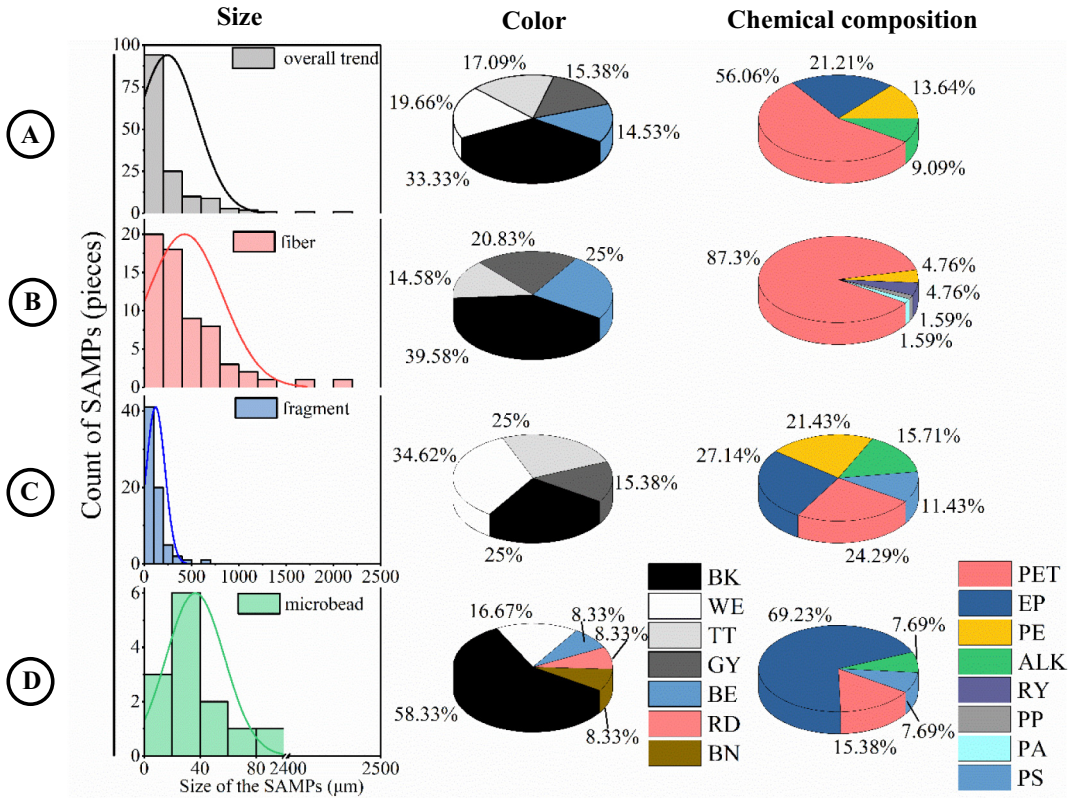

Fig. 4. Size, color, and chemical composition of the SAMPs in this study. In the figure, A illustrates the size, color, and chemical composition of the total SAMPs. B, C, and D depict the size, color, and chemical composition of the fiber-, fragment-, and microbead-shaped SAMPs. BK, WE, TT, GY, BE, RD, and BN are the percentages of black, white, transparent, gray, blue, red, and brown SAMPs, respectively. PET: polyethylene terephthalate; EP: epoxy resin; PE: polyethylene; ALK: alkyd resin; RY: rayon; PP: polypropylene; PA: polyamide; PS: polystyrene. Only the top 4 in terms of quantity of color and chemical composition were included. (For interpretation of the references to color in this figure legend, the reader is referred to the web version of this article.)

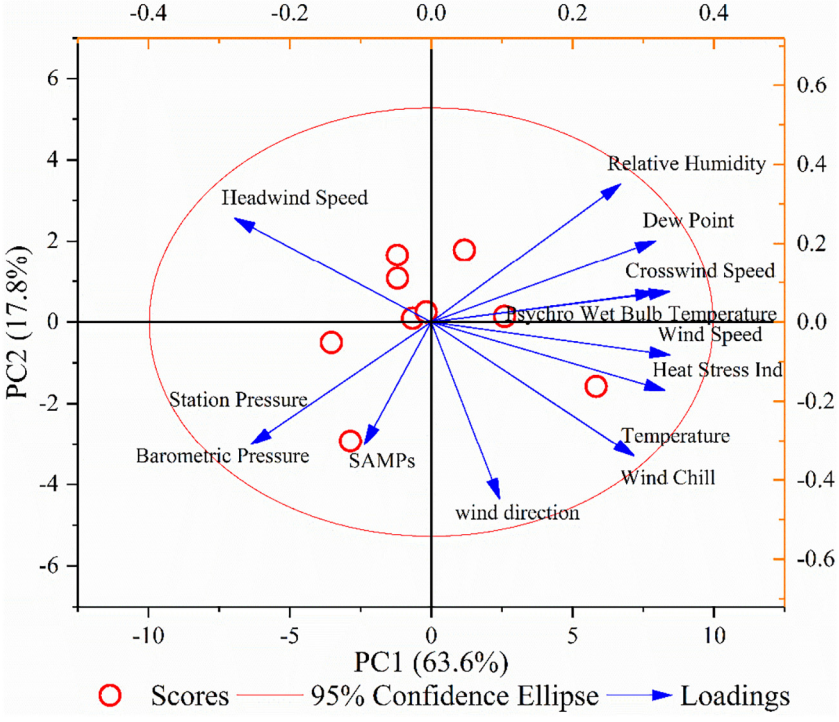

Fig. 5. Correlation between SAMP abundance and weather conditions during this investigation. In the figure, red circles and blue arrows represent the sampling information of the station and the loading variance for each weather factor on a 2-D plane, respectively, using principal component axis. (For interpretation of the references to color in this figure legend, the reader is referred to the web version of this article.)

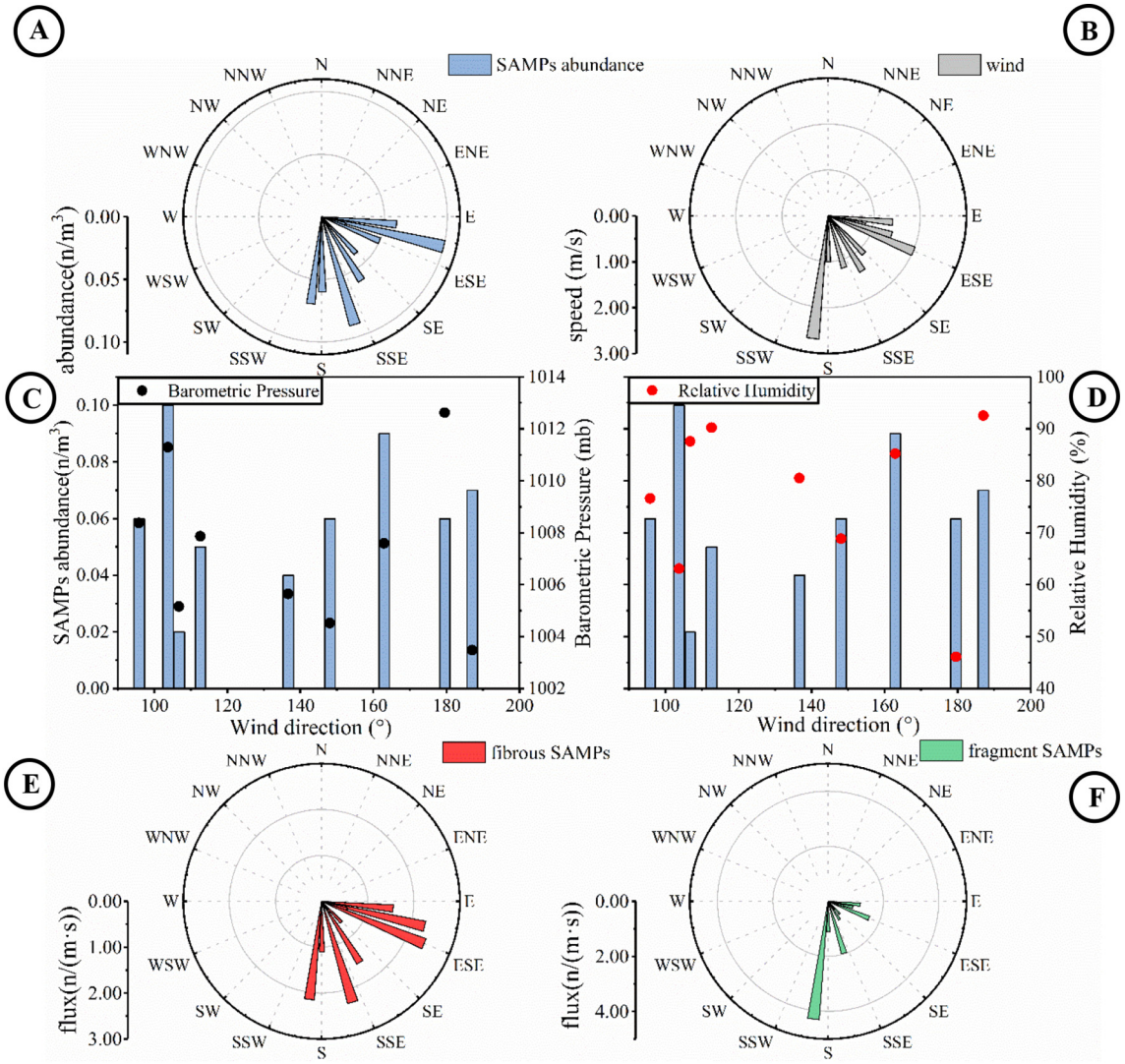

Fig. 6. Spatial distribution of SAMP abundance (A) and wind speed (B); correlation between SAMP abundance and barometric pressure (C) and relative humidity (D); estimated transport flux of fibrous (E) and fragmented SAMPs (F).

hanging it out on their balconies, favoring the direct exposure to the sunlight. In addition, some fiber-shaped SAMPs could also be produced by daily activities. During this process, the repetitive stretching of clothing made of synthetic or semi-synthetic materials could lead to the fatigue and eventual breakage of the fibers. Fragment-shaped SAMPs may originate from the breakdown of larger plastics due to long-term mechanical crushing and physical abrasion, especially from building materials and billboards. Typically, most of the aforementioned materials are made of plastics and gradually become fragile when exposed to daily sunlight and thermal effects (Cai et al., 2018; Ter Halle et al., 2016). Unlike the LDPE (low-density polyethylene) or PE microbeads in personal care products (Cheung and Fok, 2017), the microbeads observed in this study were smaller and likely originated from either additive materials designed to improve quality or raw coating materials (Burnett, 2003).

Compared to the SAMP abundance sampled during April 2018 (C. Liu et al., 2019; K. Liu et al., 2019a, 2019b), much lower abundance was found in the present study (Fig. 2-D). The significantly higher SAMP abundance in the previous study could have resulted from the much higher population density in the Putuo District (23,431 residents/km^2) compared to the Minhang District (6836 residents/km^2) (*Shanghai Statistical Yearbook*, 2018). Another possible reason could be the dilution effect of sea air; southeast winds could transport air with a relatively low abundance of SAMPs from either the adjacent area or the seaside due to the summer monsoon. A portion of the SAMPs could have been derived from deposition. In the recent report by Allen et al. (2019), 365 ± 69 n/m^3 of atmospheric MPs was found daily at a remote mountain catchment. These synthetic particles may have originated from a village 95 km away via atmospheric deposition from higher altitudes by the wind.

Table 1
Potential source of the SAMPs pollution in the study.

SAMPs shape	Polymer types	Sources	Reference
Fiber	PET, PE, RY, PP, PA	Textile (i.e. clothes, curtain and bedding)	Dris et al., 2017
Fragment	PET, EP, PE, ALK, PS	Architectural coating and weathered plastic products	Verschoor et al., 2016
Microbead	PET, EP, ALK, PS	Coasting additive	Spencer et al., 2003

Table 2
Detailed comparison of sampling methodologies and SAMP abundance in recent publications.

Study area	Sampling method	Volume per sample (m^3)	SAMP abundance (n/m^3)	Size (μm)	Fiber proportion (%)	Reference
Paris, France	Vacuum pump	5–20	0.30–1.50	50–1650	N/A	Dris et al., 2017
Asaluyeh County, Iran	Ambient filter sampler	23.60–23.93	0.30–1.10	2–100	97%	Abbasi et al., 2019
Shanghai, China	Particulate sampler	6	0.00–4.18	23–9555	67%	K. Liu et al., 2019a
Shanghai, China	Particulate sampler	72–144	0.05–0.07[a]	12–2191	43%	Present study

[a] Since a sampling volume $> 70\ m^3$ was proven to be the ideal amount for stable quantification of SAMP in the previous section, the SAMP data displayed were only from sampling volumes of filtrated air $> 70\ m^3$.

4.2. Transport implications of feature comparison and homology

Fiber-, fragment-, and microbead-shaped SAMPs were all isolated from the collected air samples, of which the majority were fibrous and fragmented SAMPs. The widespread distribution of fibrous and fragmented SAMPs has been documented in recent literature (Cai et al., 2017; K. Liu et al., 2019a), of which plastic microfibers were predominant in the air samples (Dris et al., 2016). Interestingly, in the present study a lower quantitative percentage of fibrous SAMPs but a higher percentage of fragmented SAMPs were found compared to the aforementioned reference, a finding that could stem from differences in sampling methodology and sample capacity. More SAMPs with other shapes could be unintentionally missed due to the insufficient sampling volume of air. A detailed delineation of the differences among the various sampling methods and physicochemical characteristics of SAMPs is shown in Table 2.

In this study, plastic microbeads were observed for the first time in the atmosphere, a finding that was consistent with that of a previous publication that detected them in the sediment of the Huangpu River in the area adjacent to Shanghai (Peng et al., 2018). The plastic spheres observed in the current study were also widely observed in the previous reference, especially the white-colored particles, suggesting the importance of atmospheric input. MPs with similar shapes have been detected in commercial bivalves (Li et al., 2015) and their analogous appearance suggests that these MPs could possibly be derived from the terrestrial environment via the atmosphere.

In terms of average size, the SAMPs observed in this study were smaller than the SAMPs obtained near the ground (1.7 m above the surface) (K. Liu et al., 2019a). Driven by wind, these smaller-sized SAMPs are probably more easily transported and spread to higher and more remote areas (Allen et al., 2019). In general, in this study, as size decreased, the total number of SAMPs increased, with the exception of plastic microbeads, for which the higher numbers of these airborne spherical MPs were found to be 20–40 μm in size. Dris et al. (2017) investigated the indoor and outdoor SAMPs in Paris and discovered a similar size distribution, in which the number of SAMPs decreased for the larger-sized plastic particles.

A similar but slightly different size composition of SAMPs was observed compared to the depositional MPs in Yantai City, China, in which over half of these synthetic particles were < 500 μm (Zhou et al., 2017). In the current investigation, 87% of the total SAMPs by quantity were < 500 μm and SAMPs with sizes < 330 μm comprised 80% of these atmospheric MPs. After entering the ocean, these MPs may possibly be underestimated when using the manta trawl (typically with a 330-μm mesh size).

The resulting data were similar to those of a previous study by C. Liu et al. (2019) and K. Liu et al. (2019a, 2019b), in which black, blue, yellow, green, transparent, and brown PET-type SAMPs were also identified from atmospheric samples collected in the Putuo District of Shanghai. Different from previous research, in current work, white (3 fibers; 18 fragments; 2 microbeads), pink (3 fibers) and purple (1 fiber) colored SAMPs were found, which possibly has a potential connection with local architectures and textile types. Transparent plastic fragments with PS polymer composition could have originated from weathered plastic debris near the study area. Hu et al. (2018) reported MP pollution in the aquatic environment of the Yangtze River Delta, where transparent PS MPs were also observed in the water and sediment.

4.3. Implications for human health and the ecosystem

SAMPs, as a particulate POPs, can be inhaled and pose a potential threat to humans. Inhaled MPs can directly contact respiratory organs and accumulate in the human lung, resulting in chronic symptoms. Recent publications have reviewed the diagnosed diseases associated with plastics or plastic derivatives (Prata, 2018). To date, however, there has not been any type of appropriate assessment modeling that is fully suitable for SAMPs. Although several studies have estimated the potential health impact caused by MPs from indoor and outdoor dust (C. Liu et al., 2019; Abbasi et al., 2019), the SAMP assessments have possibly led to ambiguous results due to indirect sampling. Given the shortage of potential health impact assessments from SAMPs, the general framework for future assessment was suggested and a schematic diagram presented in Fig. 7. The biogeochemical characteristics of both SAMPs and human factors were fully considered. Primarily, the abundance or concentration of SAMPs probably exerts a certain influence on ingested organisms, a relationship that has been verified by many dose-based toxicological experiments (Bour et al., 2018). In addition, since the physicochemical properties of MPs may influence the interaction with organisms, physical appearance, and polymer type should also be considered. Previous research has proven that the physicochemical properties of MPs can influence their bioavailability. During an exposure experiment, Li et al. (2019) discovered that *Corbicula fluminea* preferred to ingest the smaller-sized plastic microfibers of polyester. Potential health risks may be aggravated by smaller-sized SAMPs, which pose more of a threat to aquatic organisms than larger SAMPs (Jeong et al., 2016). Lee et al. (2013) observed the size-dependent effect of MPs on marine copepods, finding that smaller-sized MPs can impair copepod fecundity.

MPs can be the carriers of persistent organic pollutants (POPs) (Andrady, 2011) as well as some pathogens (Jiang et al., 2018), potentially causing more severe physical reactions. Meanwhile, plasticizers, antioxidants and slip agents, as typical additives in plastics could more possibly lead to toxic effect than plastics itself (Hahladakis et al., 2018). For example, high concentrations of organophosphorus esters and phthalates have been identified on the beached microplastics, especially on PP flake and PS foam (Zhang et al., 2018).

Plastic debris colonized by pathogens have been reported to exhibit a close relationship with coral disease, with the possibility of disease 4–89% greater than the plastics-free condition (Lamb et al., 2018). POPs adhered to MPs could possibly be leached and translocated when subjected to physiological stress from organisms once ingested (Wardrop et al., 2016). Moreover, these suspended MPs easily receive sufficient UV irradiation, resulting in the acceleration of the fragmentation process and an expansion specific surface area (Lambert and Wagner, 2016). Thus, a higher concentration of gaseous POPs would be more easily absorbed on these suspended MPs. Meanwhile, some organic matter would be generated from the weathered MPs, which could potentially alter the biogeochemical cycle of global carbon (Romera-Castillo et al., 2018). Compared with MPs in the aquatic environment, these airborne particles would probably receive more intense UV

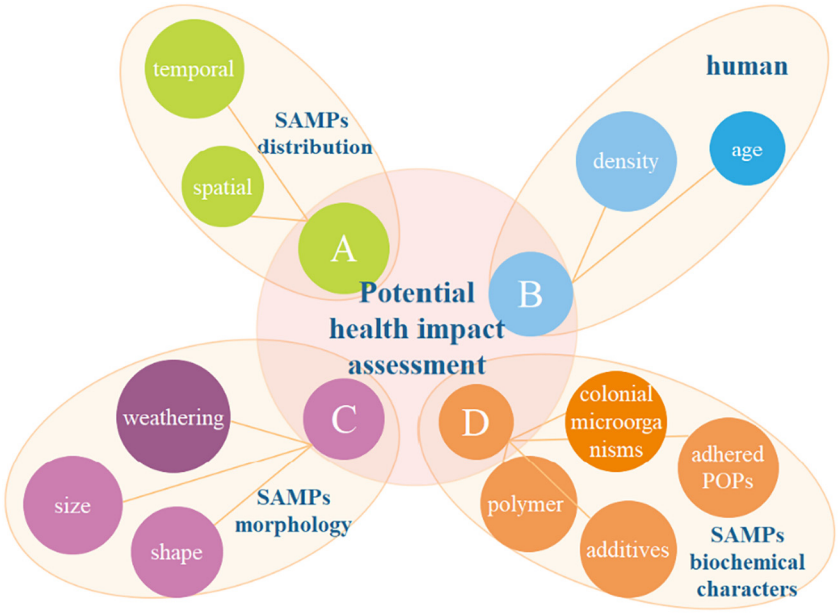

Fig. 7. Framework of potential health impacts from SAMPs.

irradiation, leading to the possible leaching of more organic matter in gaseous form, a phenomenon that may have long-term impacts on global climate.

5. Conclusions

Although SAMPs have been recognized as a vital source for marine MP pollution and may adversely impact humans via inhalation, SAMPs from the atmosphere have possibly been either underestimated or overestimated due to a lack of proper sampling methodology. Until the realistic SAMP abundance is quantified, any potential ecological or health assessment will be open to criticism for using an ambiguous dataset. In order to address this issue, this study was the first to offer a sampling methodology for the stable quantification of SAMPs. In addition, the relationship between SAMP abundance and the sampling volume of filtrated air was explored. A significant logarithmic regression between the average abundance and volume of the sampled air was discovered, implying the necessity of sufficient sampling volume. Based on our latest findings, a filtrated air sampling volume of at least 70 m^3 is required and recommended for SAMP quantification. Further PCA and spatial analysis demonstrated the relationship between SAMPs and environmental parameters in terms of the June distribution pattern of SAMPs in Shanghai. Our findings also imply that SAMPs may originate not only from lateral transport but also from vertical deposition from higher altitudes. Based on our modeling, the general transport flux of SAMPs during June in Shanghai was tentatively estimated, ranging from 9.94×10^4 n/(m·d)–6.52×10^5 n/(m·d), with a mean of $3.00 \pm 1.58 \times 10^5$ n/(m·d). These considerable amounts of SAMPs in Shanghai warrant further investigation. Given the complex behavior of SAMPs and their potential impacts on human health and climate, a more detailed and inclusive assessment is urgently needed. Our proposed framework could serve as the baseline for future assessments.

Supplementary data to this article can be found online at https://doi.org/10.1016/j.envint.2019.105127.

Declaration of competing interest

The authors declare no competing financial interests.

Acknowledgments

This research was funded by the National Key Research and Development Program (2016YFC1402205), National Natural Science Fund of China (41676190), and the ECNU Academic Innovation Promotion Program for Excellent Doctoral Students (YBNLTS2019-007). We would like to express our sincere thanks to the anonymous reviewers and dedicated editors for their invaluable opinions and contributions, which greatly improved the quality of this manuscript.

References

Abbasi, S., Keshavarzi, B., Moore, F., Turner, A., Kelly, F.J., Dominguez, A.O., Jaafarzadeh, N., 2019. Distribution and potential health impacts of microplastics and microrubbers in air and street dusts from Asaluyeh County, Iran. Environ. Pollut. 244, 153–164. https://doi.org/10.1016/j.envpol.2018.10.039.

Allen, S., Allen, D., Phoenix, V. R., Le Roux, G., Jiménez, P. D., Simonneau, A., … & Galop, D. 2019. Atmospheric transport and deposition of microplastics in a remote mountain catchment. Nat. Geosci., 12(5), 339. doi:https://doi.org/10.1038/s41561-019-0335-5.

Andrady, A.L., 2011. Microplastics in the marine environment. Mar. Pollut. Bull. 62 (8), 1596–1605. https://doi.org/10.1016/j.marpolbul.2011.05.030.

Bour, A., Haarr, A., Keiter, S., Hylland, K., 2018. Environmentally relevant microplastic exposure affects sediment-dwelling bivalves. Environ. Pollut. 236, 652–660. https://doi.org/10.1016/j.envpol.2018.02.006.

Burnett, D., 2003. U.S. microbead coating composition and methods. No 9 (/886), 646.

Cai, L., Wang, J., Peng, J., Tan, Z., Zhan, Z., Tan, X., Chen, Q., 2017. Characteristic of microplastics in the atmospheric fallout from Dongguan city, China: preliminary research and first evidence. Environ. Sci. Pollut. Res. 24 (32), 24928–24935. https://doi.org/10.1007/s11356-017-0116-x.

Cai, L., Wang, J., Peng, J., Wu, Z., Tan, X., 2018. Observation of the degradation of three types of plastic pellets exposed to UV irradiation in three different environments. Sci. Total Environ. 628, 740–747. https://doi.org/10.1016/j.scitotenv.2018.02.079.

Carbery, M., O'Connor, W., Palanisami, T., 2018. Trophic transfer of microplastics and mixed contaminants in the marine food web and implications for human health. Environ. Int. 115, 400–409. https://doi.org/10.1016/j.envint.2018.03.007.

Cheung, P.K., Fok, L., 2017. Characterisation of plastic microbeads in facial scrubs and their estimated emissions in Mainland China. Water Res. 122, 53–61. https://doi.org/10.1016/j.watres.2017.05.053.

Dris, R., Gasperi, J., Saad, M., Mirande, C., Tassin, B., 2016. Synthetic fibers in atmospheric fallout: a source of microplastics in the environment? Mar. Pollut. Bull. 104 (1–2), 290–293. https://doi.org/10.1016/j.marpolbul.2016.01.006.

Dris, R., Gasperi, J., Mirande, C., Mandin, C., Guerrouache, M., Langlois, V., Tassin, B., 2017. A first overview of textile fibers, including microplastics, in indoor and outdoor environments. Environ. Pollut. 221, 453–458. https://doi.org/10.1016/j.envpol.2016.12.013.

Hahladakis, J.N., Velis, C.A., Weber, R., Iacovidou, E., Purnell, P., 2018. An overview of chemical additives present in plastics: migration, release, fate and environmental impact during their use, disposal and recycling. J. Hazard. Mater. 344, 179–199. https://doi.org/10.1016/j.jhazmat.2017.10.014.

Hu, L., Chernick, M., Hinton, D.E., Shi, H., 2018. Microplastics in small waterbodies and tadpoles from Yangtze River Delta, China. Environ. Sci. Technol. 52 (15), 8885–8893. https://doi.org/10.1021/acs.est.8b02279.

Jeong, C.B., Won, E.J., Kang, H.M., Lee, M.C., Hwang, D.S., Hwang, U.K., Lee, J.S., 2016. Microplastic size-dependent toxicity, oxidative stress induction, and p-JNK and p-p38 activation in the monogonont rotifer (*Brachionus koreanus*). Environ. Sci. Technol. 50 (16), 8849–8857. https://doi.org/10.1021/acs.est.6b01441.

Jiang, P., Zhao, S., Zhu, L., Li, D., 2018. Microplastic-associated bacterial assemblages in the intertidal zone of the Yangtze Estuary. Sci. Total Environ. 624, 48–54. https://doi.org/10.1016/j.scitotenv.2017.12.105.

Kan, H., Chen, R., Tong, S., 2012. Ambient air pollution, climate change, and population health in China. Environ. Int. 42, 10–19. https://doi.org/10.1016/j.envint.2011.03.003.

Lamb, J.B., Willis, B.L., Fiorenza, E.A., Couch, C.S., Howard, R., Rader, D.N., Harvell, C.D., 2018. Plastic waste associated with disease on coral reefs. Science 359 (6374), 460–462. https://doi.org/10.1126/science.aar3320.

Lambert, S., Wagner, M., 2016. Characterisation of nanoplastics during the degradation of polystyrene. Chemosphere 145, 265–268. https://doi.org/10.1016/j.chemosphere.2015.11.078.

Law, K.L., Thompson, R.C., 2014. Microplastics in the seas. Science 345 (6193), 144–145. https://doi.org/10.1126/science.1254065.

Lee, K.W., Shim, W.J., Kwon, O.Y., Kang, J.H., 2013. Size-dependent effects of micro polystyrene particles in the marine copepod *Tigriopus japonicus*. Environ. Sci. Technol. 47 (19), 11278–11283. https://doi.org/10.1021/es401932b.

Li, J., Yang, D., Li, L., Jabeen, K., Shi, H., 2015. Microplastics in commercial bivalves from China. Environ. Pollut. 207, 190–195. https://doi.org/10.1016/j.envpol.2015.09.018.

Li, L., Su, L., Cai, H., Rochman, C.M., Li, Q., Kolandhasamy, P., Shi, H., 2019. The uptake of microfibers by freshwater Asian clams (*Corbicula fluminea*) varies based upon physicochemical properties. Chemosphere 221, 107–114. https://doi.org/10.1016/j.chemosphere.2019.01.024.

Liu, C., Li, J., Zhang, Y., Wang, L., Deng, J., Gao, Y., Sun, H., 2019a. Widespread distribution of PET and PC microplastics in dust in urban China and their estimated human exposure. Environ. Int. 128, 116–124. https://doi.org/10.1016/j.envint.2019.04.024.

Liu, K., Wang, X., Fang, T., Xu, P., Zhu, L., Li, D., 2019b. Source and potential risk assessment of suspended atmospheric microplastics in Shanghai. Sci. Total Environ. 675, 462–471. https://doi.org/10.1016/j.scitotenv.2019.04.110.

Liu, K., Zhang, F., Song, Z., Zong, C., Wei, N., Li, D., 2019c. A novel method enabling the accurate quantification of microplastics in the water column of deep ocean. Mar. Pollut. Bull. 146, 462–465. https://doi.org/10.1016/j.marpolbul.2019.07.008.

Ostle, C., Thompson, R.C., Broughton, D., Gregory, L., Wootton, M., Johns, D.G., 2019. The rise in ocean plastics evidenced from a 60-year time series. Nat. Commun. 10 (1), 1622. https://doi.org/10.1038/s41467-019-09506-1.

Peeken, I., Primpke, S., Beyer, B., Gütermann, J., Katlein, C., Krumpen, T., Gerdts, G., 2018. Arctic sea ice is an important temporal sink and means of transport for microplastic. Nat. Commun. 9 (1), 1505. https://doi.org/10.1038/s41467-018-03825-5.

Peng, G., Xu, P., Zhu, B., Bai, M., Li, D., 2018. Microplastics in freshwater river sediments in Shanghai, China: a case study of risk assessment in mega-cities. Environ. Pollut. 234, 448–456. https://doi.org/10.1016/j.envpol.2017.11.034.

Prata, J.C., 2018. Airborne microplastics: consequences to human health? Environ. Pollut. 234, 115–126. https://doi.org/10.1016/j.envpol.2017.11.043.

Romera-Castillo, C., Pinto, M., Langer, T.M., Álvarez-Salgado, X.A., Herndl, G.J., 2018. Dissolved organic carbon leaching from plastics stimulates microbial activity in the ocean. Nat. Commun. 9 (1), 1430. https://doi.org/10.1038/s41467-018-03798-5.

Setälä, O., Fleming-Lehtinen, V., Lehtiniemi, M., 2014. Ingestion and transfer of microplastics in the planktonic food web. Environ. Pollut. 185, 77–83. https://doi.org/10.1016/j.envpol.2013.10.013.

Shanghai Statistical Yearbook. http://www.stats-sh.gov.cn/html/sjfb/201901/1003014.html.

Song, Y.K., Hong, S.H., Jang, M., Han, G.M., Jung, S.W., Shim, W.J., 2017. Combined effects of UV exposure duration and mechanical abrasion on microplastic fragmentation by polymer type. Environ. Sci. Technol. 51 (8), 4368–4376. https://doi.org/10.1021/acs.est.6b06155.

Spencer, A.B., Andrews, J.W., Gary, D.T.I., 2003. U.S. Patent No. 6,525,111. U.S. Patent and Trademark Office, Washington, DC.

Su, L., Deng, H., Li, B., Chen, Q., Pettigrove, V., Wu, C., Shi, H., 2019. The occurrence of microplastic in specific organs in commercially caught fishes from coast and estuary area of east China. J. Hazard. Mater. 365, 716–724. https://doi.org/10.1016/j.jhazmat.2018.11.024.

Ter Halle, A., Ladirat, L., Gendre, X., Goudouneche, D., Pusineri, C., Routaboul, C., Perez, E., 2016. Understanding the fragmentation pattern of marine plastic debris. Environ. Sci. Technol. 50 (11), 5668–5675. https://doi.org/10.1021/acs.est.6b00594.

Verschoor, A., De Poorter, L., Dröge, R., Kuenen, J., de Valk, E., 2016. Emission of Microplastics and Potential Mitigation Measures: Abrasive Cleaning Agents. Paints and Tyre Wear.

Wardrop, P., Shimeta, J., Nugegoda, D., Morrison, P.D., Miranda, A., Tang, M., Clarke, B.O., 2016. Chemical pollutants sorbed to ingested microbeads from personal care products accumulate in fish. Environ. Sci. Technol. 50 (7), 4037–4044. https://doi.org/10.1021/acs.est.5b06280.

Zhang, H., Zhou, Q., Xie, Z., Zhou, Y., Tu, C., Fu, C., Luo, Y., 2018. Occurrences of organophosphorus esters and phthalates in the microplastics from the coastal beaches in north China. Sci. Total Environ. 616, 1505–1512. https://doi.org/10.1016/j.scitotenv.2017.10.163.

Zhao, S., Zhu, L., Li, D., 2016. Microscopic anthropogenic litter in terrestrial birds from Shanghai, China: not only plastics but also natural fibers. Sci. Total Environ. 550, 1110–1115. https://doi.org/10.1016/j.scitotenv.2016.01.112.

Zhao, S., Danley, M., Ward, J.E., Li, D., Mincer, T.J., 2017. An approach for extraction, characterization and quantitation of microplastic in natural marine snow using Raman microscopy. Anal. Methods 9 (9), 1470–1478. https://doi.org/10.1039/c6ay02302a.

Zhao, S., Ward, J.E., Danley, M., Mincer, T.J., 2018. Field-based evidence for microplastic in marine aggregates and mussels: implications for trophic transfer. Environ. Sci. Technol. 52 (19), 11038–11048. https://doi.org/10.1021/acs.est.8b03467.

Zhou, Q., Tian, C., Luo, Y., 2017. Various forms and deposition fluxes of microplastics identified in the coastal urban atmosphere. Chin. Sci. Bull. 62 (33), 3902–3910. https://doi.org/10.1360/N972017-00956.